

A SLIDING-MODE BASED SMOOTH ADAPTIVE ROBUST CONTROLLER FOR FRICTION COMPENSATION

GANGBING SONG^{1*}, LILONG CAI², YIPING WANG³ AND RICHARD W. LONGMAN³

¹*Department of Aeronautics and Astronautics, U.S. Naval Postgraduate School, Monterey, CA 93943, U.S.A*

²*Department of Mechanical Engineering, Hong Kong University of Science and Technology, Kowloon, Hong Kong*

³*Department of Mechanical Engineering, Columbia University, New York, NY 10027, U.S.A.*

SUMMARY

In this paper, a new approach employing both adaptive and robust methodologies is proposed for stick–slip friction compensation for tracking control of a one degree-of-freedom DC-motor system. It is well known that the major components of friction are Coulomb force, viscous force, exponential force (used to model the downward bend of friction at low velocity) and position-dependent force. Viscous force is linear and Coulomb force is linear in parameter; thus, these two forces can be compensated for by adaptive feedforward cancellation. Meanwhile, the latter two forces, which are neither linear nor linear in parameters, can only be partially compensated for by adaptive feedforward cancellation. Therefore, a robust compensator with an embedded adaptive law to ‘learn’ the upper bounding function on-line is proposed to compensate the uncanceled exponential and position-dependent friction. Lyapunov’s direct method is utilized to prove the globally asymptotic stability of the servo-system under the proposed friction compensation method. Numerical simulations are presented as illustrations. © 1998 John Wiley & Sons, Ltd.

Key words: sliding-mode control; friction compensation; adaptive robust control; nonlinear control; stick–slip friction

1. INTRODUCTION

Stick–slip friction exists in virtually all mechanical systems. Owing to its discontinuity at zero velocity and the downward bend of the friction torque at low velocity, stick–slip friction is often responsible for positioning inaccuracy and motion intermittence in servo-mechanisms.

Conventional feedback control methods cannot guarantee satisfactory results in the presence of stick–slip friction. In the regulator problem, a traditional PD controller will not achieve satisfactory performance because it results in a steady-state error. The error may be reduced by increasing the proportional gain, but high gain controllers have drawbacks, such as causing system instability when the drive train is compliant. PID controllers may provoke the generation of limit cycles, thus resulting in motion intermittence.¹

This paper was recommended for publication by editor M. D. Di Benedetto

*Correspondence to: G. Song, Department of Aeronautics and Astronautics, U.S. Naval Postgraduate School, Monterey, CA 93943, U.S.A.

The method of feedforward cancellation can be used to eliminate the detrimental effects of friction, but its use requires an accurate friction model which is rarely available. Adaptive friction compensation schemes have been proposed to compensate for imprecisely known nonlinear friction, but they are usually based on linearized models or models with linearized parameters. Robust controllers have been developed to strengthen the compensation for nonlinear friction. Canudas de Wit and Loard Scront,² for example, designed a linear compensator 'robustifying' the closed-loop system in the presence of inexact friction compensation induced by adaptive transients and other external disturbances. Southward, Radeliffe and MacCluer¹ implemented a robust nonlinear compensator for regulation of a single degree-of-freedom object with stick-slip friction, and achieved asymptotic stability. However, it produces a bang-bang force in the region near the desired reference, causing extra acceleration disturbances, which are often undesirable. Cai and Song³ proposed a smooth robust nonlinear controller for regulation of robot manipulators with joint stick-slip friction, ensuring both high precision and smooth motion. In later work by Cai and Song⁴ stick-slip friction compensation algorithms have been developed for robot tracking control and global asymptotic stability of the closed-loop system with smooth control input. However, the proposed robust controllers, like other commonly used ones, require knowledge of upper bounds (or upper bounding functions) for uncertainties (including stick-slip friction) in order to guarantee closed-loop stability. This requirement sometimes restricts the application of robust controllers or results in poor performance when the upper bounds are not properly estimated.

The aim of this paper is to provide a new scheme to effectively compensate for stick-slip friction for tracking control of one degree-of-freedom (DOF) servo-mechanisms with uncertain parameters. The scheme guarantees high precision, it guarantees smoothness of motion, it is robust to uncertainty in parameters and friction, and it relaxes the usual requirement of robust control of having a known upper bound on the uncertainties. Thus, it is applicable to a broader class of systems than pure robust control methods.

The approach used here employs variable structure concepts, specifically, the sliding mode method as in Slotine and Li.⁵ One of the advantages of the method is that there is no need for acceleration estimation or measurement when implementing the developed tracking controller. In order to force the system dynamics onto the sliding mode, we use the smooth robust controller with a time-varying hyperbolic tangent function, which switches around the sliding surface in a smooth manner, as developed in Cai and Abdalla,⁶ and Cai and Song.³ The smooth controller has advantages over conventional robust controllers, such as the bang-bang (discontinuous type) and the saturation (continuous type) controllers, in the sense that both asymptotic stability of the closed-loop system and smooth control action can be guaranteed simultaneously.

The proposed controller consists of three main parts: 1. feedforward terms computed based on the known dynamic structure of the servo mechanism together with part of a stick-slip friction model. The feedforward terms with parameter linearity are tuned on line according to adaptive laws. 2. A linear PD feedback. 3. A robust controller designed to compensate for the uncancelled friction due to inexact estimation of the downward friction curve at low velocity and to the position-dependent friction force, both of which cannot be compensated for by the above adaptive feedforward compensation. The requirement of knowing an upper bound on the uncertainties when employing robust controllers is relaxed by using an additional adaptive law to tune the upper bounding function.

Lyapunov's direct method is used to prove the global asymptotic stability of the closed-loop system. Numerical simulations of applying the proposed control scheme to a 1-DOF DC-motor

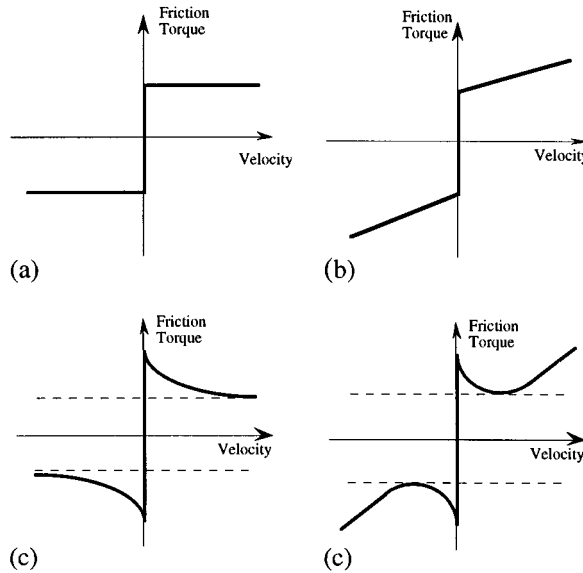


Figure 1. Commonly used stick-slip friction models

system show that stick-slip friction can be effectively compensated for and the desired trajectory can be followed precisely.

2. MODELLING OF STICK-SLIP FRICTION

Stick-slip friction is present in any elements involving relative motion, such as gears, pulleys, bearings and DC motors. Stick-slip friction is generally described as a composite of two different processes: the static process when an object is stationary (no sliding is involved) and likely to move under certain applied torque, and the dynamic process when sliding is involved.

The static process is characterized by the maximum static torque (or breakaway torque), under which static state remains and the magnitude of the static friction force is equal to that of the applied force.

The slipping process is relatively complicated. Many factors affect the friction torque, such as lubrication, velocity, position and forces orthogonal to the motion surface. In practice, the downward bend of friction force at low velocity, often called the Stribeck effect^{7,8} i.e., friction forces decrease with increasing velocity at low velocity, has been observed. Frictional lags between velocity reversals, i.e., hysteresis, has also been noticed.

Slipping torque is usually modelled as a linear combination of Coulomb torque, viscous torque, exponential torque^{8,9} used to represent the Stribeck effect, and position¹⁰ dependent components. Some commonly used friction models are shown in Figure 1(a)–(d).

In this paper, a mathematical formulation of the stick-slip friction (denoted by τ_{fm}) including Coulomb friction, viscous friction, exponential friction and position dependent friction is proposed as

$$\tau_{fm} = \tau_{stm} \text{sgn}(\dot{q}) + k_{vism} \dot{q} - \tau_{em} (1 - e^{-(\tau_0/|\dot{q}|)}) \text{sgn}(\dot{q}) + \tau_{pm} \text{sgn}(\dot{q}) + [1 - \text{sgn}(|\dot{q}|)] \tau_i \quad (1)$$

where k_{vism} is the coefficient of viscous friction; τ_{stm} represents the maximum static friction torque or breakaway torque; $\text{sgn}(\bullet)$ is the sign function; $-\tau_{\text{em}}(1 - e^{-(T_0/|\dot{q}|)})\text{sgn}(\dot{q})$ represents the Stribeck effect and T_0 is a positive constant; τ_i is the input torque; $[1 - \text{sgn}(|\dot{q}|)]\tau_i$ stands for the static friction force whose magnitude is equal to the applied force; τ_{pm} , the position-dependent friction torque, can be modelled as

$$\tau_{\text{pm}} = \beta_{1\text{m}} \sin(\beta_2 q + \beta_3) \quad (2)$$

where $\beta_{1\text{m}}$, β_2 and β_3 are constants.

It is noticed that in equations (1) and (2) the viscous friction is linear, while the Coulomb friction is linear in parameter; whereas, the exponential force and the position-dependent friction are neither linear nor parametric linear.

The friction model (1) does not include the hysteresis effect. However, as will be shown later, the control method developed in this paper will be able to ensure position tracking error to converge to zero in the presence of the hysteresis effect.

3. SYSTEM MODEL

We consider DC-motor systems with stick-slip friction, since DC motors are the most commonly used precision servo-systems in present-day industry. Shown in the following is a dynamic model of permanent magnet DC motors.

$$J_{\text{m}} \ddot{q}(t) + \frac{k_{\text{b}} k_{\text{m}}}{R} \dot{q}(t) + \tau_{\text{fm}} = k_{\text{m}} i_{\text{m}} \quad (3)$$

where $q(t)$ is the rotor angular position; J_{m} is the total moment of inertia reflected to the rotor axis; R and i_{m} denote the armature resistance and current, respectively; k_{b} and k_{m} stand for the back emf constant and motor torque constant, respectively; τ_{fm} is the stick-slip friction.

Dividing both sides of equation (3) by k_{m} gives

$$J \ddot{q}(t) + B \dot{q}(t) + \tau_{\text{f}} = i \quad (4)$$

where $J = J_{\text{m}}/k_{\text{m}}$, $B = k_{\text{b}}/R$ and $\tau_{\text{f}} = \tau_{\text{fm}}/k_{\text{m}}$.

The friction torque τ_{f} in (4) can be expressed as

$$\tau_{\text{f}} = \tau_{\text{st}} \text{sgn}(\dot{q}) + k_{\text{vis}} \dot{q} - \tau_{\text{e}} (1 - e^{-(T_0/|\dot{q}|)}) \text{sgn}(\dot{q}) + \tau_{\text{p}} \text{sgn}(|\dot{q}|) + [1 - \text{sgn}(\dot{q})] i \quad (5)$$

where τ_{st} , k_{vis} , τ_{e} and τ_{p} are obtained by dividing τ_{stm} , k_{vism} , τ_{em} and τ_{pm} by k_{m} , respectively.

Owing to system uncertainty, system parameters in (4) and friction parameters in (5) may not be known exactly for control design.

4. CONTROL DESIGN

Adaptive feedforward cancellation is used to compensate for viscous and Coulomb friction forces based on the fact that they are linear or parametric linear. The exponential and position-dependent forces, which are nonlinear or nonlinear in parameters, cannot be adaptively feedforward cancelled. Nevertheless, it will be shown that the uncanceled residual is bounded, and thus, a robust compensator is designed to compensate for this residual. Based on the work by Lewis,

Abdallah and Dawson,¹¹ an adaptation law is embedded into the robust compensator to ‘learn’ an upper bounding function. The control design will take advantage of the so-called sliding-surface method as presented in Slotine and Li,⁵ so that there is no need to measure or estimate the acceleration when implementing the controller.

Definitions

The control error and error derivative are

$$e = q - q^d, \dot{e} = \dot{q} - \dot{q}^d \tag{6}$$

where the items with the superscript ‘d’ represent their corresponding desired values. Define v and \dot{v} by

$$v = \dot{q}^d - \lambda e, \dot{v} = \ddot{q}^d - \lambda \dot{e} \tag{7}$$

and r and \dot{r} by

$$r = \dot{q} - v = \dot{e} + \lambda e, \dot{r} = \ddot{q} - \dot{v} = \ddot{e} + \lambda \dot{e} \tag{8}$$

where λ is a constant diagonal matrix of positive gains. The sliding surface is given by $r = 0$.

The controller

Utilizing the dynamic structure shown in equations (4) and (5), the controller for tracking control of the DC-motor system with stick–slip friction is proposed as

$$i = \hat{J}\dot{v} + \hat{B}v + \hat{k}_{vis}v + \hat{\tau}_{st}\text{sgn}(\dot{q}) - \hat{\tau}_e(1 - e^{-(\hat{\tau}_e|\dot{q}|)})\text{sgn}(\dot{q}) + \hat{\tau}_{st}(1 - \text{sgn}(|\dot{q}|))(1 - \text{sgn}(|r|)) - K_D r - \hat{\rho}K_T \tanh[(a + bt)r] \tag{9}$$

The K_D , K_T , a and b are positive constants, and $K_T > 1$. Terms with a circumflex ‘ $\hat{\cdot}$ ’ represent their corresponding estimates. The \hat{J} , $\hat{B} + \hat{K}_{vis}$ and $\hat{\tau}_{st}$ are estimates of parameters appearing linearly and are updated during the control process. The $\hat{\rho}$ is an estimate of an upper bound on the uncertainty residual for terms nonlinear in parameters, and is also adaptively updated. Note that there are two terms involving the estimate of static friction $\hat{\tau}_{st}$, the first one applies when there is relative motion and the second applies when there is no relative motion. The proposed control scheme is illustrated by the block diagram (Figure 2).

Adaptation for breakaway

When the maximum static friction torque is underestimated, sticking occurs. The adaptive law to update $\hat{\tau}_{st}$ in order to produce breakaway is designed as

$$\dot{\hat{\tau}}_{st} = k_\tau(1 - \text{sgn}(|\dot{q}|))|r| \tag{10}$$

where k_τ is a positive constant. This is the only dynamics involved during sticking when the driving torque is less than the breakaway torque and is balanced by static friction. This law ensures breakaway as long as $|r| \neq 0$, and when it is equal to zero the system is in sliding mode, which guarantees convergence to zero error. The following sections give the update rules for all of the other parameters of the control law, as well as an updating rule for $\hat{\tau}_{st}$ that replaces (10) when relative motion is present.

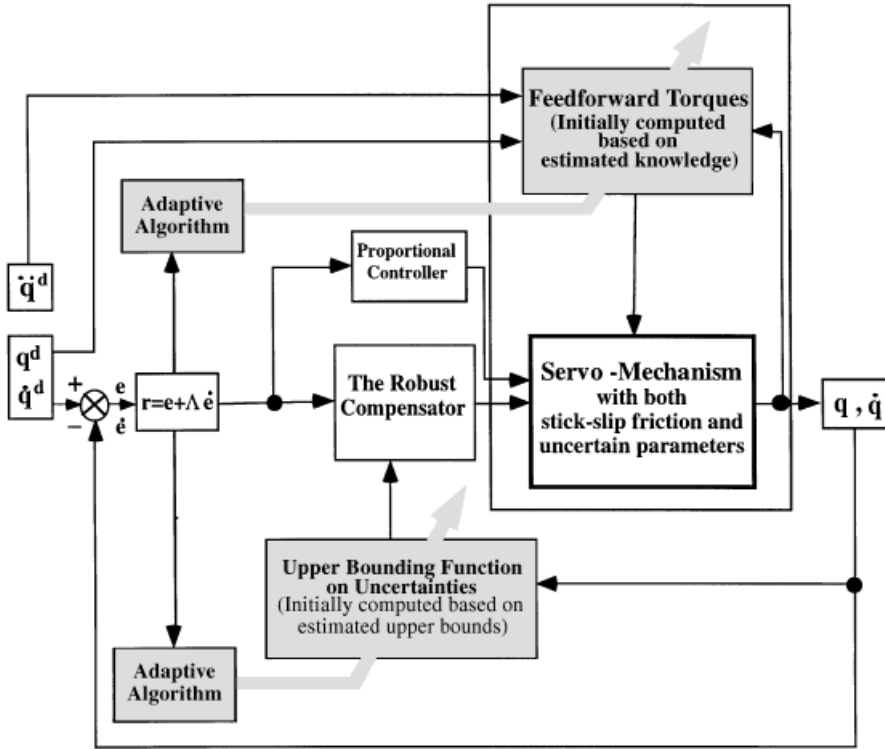


Figure 2. The block diagram illustrating smooth adaptive robust friction compensation

Adaptation to the parameters appearing linearly

Equation (9) can be rewritten to collect together the parameters that appear linearly

$$i = \mathbf{Y}\hat{\Phi} + \hat{\tau}_{st}(1 - \text{sgn}(|\dot{q}|))(1 - \text{sgn}(|r|)) - K_D r - \hat{\tau}_c(1 - e^{-\hat{\tau}_c|\dot{q}|})\text{sgn}(\dot{q}) - \hat{\rho}K_T \tanh[a + bt]r \tag{11}$$

where

$$\mathbf{Y} = [\dot{v} \ v \ \text{sgn}(\dot{q})]$$

$$\hat{\Phi} = [\hat{J} \ \hat{B} + \hat{k}_{vis} \ \hat{\tau}_{st}]^T$$

Then the adaptive law to update $\hat{\Phi}$ is

$$\dot{\hat{\Phi}} = -\mathbf{\Omega}_1 \mathbf{Y}^T r \tag{12}$$

where $\mathbf{\Omega}_1 \in \mathbf{R}^{3 \times 3}$ is a diagonal matrix with positive gains (the last column is deleted in favour of (10) when there is no motion).

Modelling of the upper bounding function

Substituting (11) and (5) into (4) and utilizing equation (8), we have the equation of motion

$$J\ddot{r} + (B + k_{vis})r + K_D r = \mathbf{Y}\hat{\Phi} + \omega - \hat{\rho}K_T \tanh[(a + bt)r] \tag{13}$$

where the terms with a tilde ‘ \sim ’ represent the differences between their corresponding estimates and real values, and ω is the uncanceled residual of the exponential and position-dependent friction force, given by

$$\begin{aligned} \omega &= -\beta_1 \sin(\beta_2 q + \beta_3) \operatorname{sgn}(\dot{q}) + \operatorname{sgn}(\dot{q}) \{ \hat{\tau}_e e^{-\hat{T}_0 |\dot{q}|} - \tau_e e^{-T_0 |\dot{q}|} - \tilde{\tau}_e \} \\ &= -\beta_1 \sin(\beta_2 q + \beta_3) \operatorname{sgn}(\dot{q}) + \operatorname{sgn}(\dot{q}) \{ \hat{\tau}_e e^{-\hat{T}_0 |\dot{q}|} - \tau_e e^{-\hat{T}_0 |\dot{q}|} e^{\tilde{T}_0 |\dot{q}|} - \tilde{\tau}_e \} \end{aligned} \tag{14}$$

It will be shown, in the next section, that there exist constants $\alpha_1, \alpha_2, \alpha_3$ and α_4 such that this residual is bounded by

$$\rho \geq |\omega| \tag{15}$$

where

$$\rho = \alpha_1 + \alpha_2 e^{-\hat{T}_0 |\dot{q}|} + \alpha_3 |\dot{q}| e^{-\hat{T}_0 |\dot{q}|} + \alpha_4 |\dot{q}|^2 e^{-\hat{T}_0 |\dot{q}|} \tag{16}$$

In matrix form, this upper bounding function ρ which is linear in parameters can be written

$$\rho = \mathbf{X}\Psi \tag{17}$$

where

$$\begin{aligned} \mathbf{X} &= [1 \quad e^{-\hat{T}_0 |\dot{q}|} \quad |\dot{q}| e^{-\hat{T}_0 |\dot{q}|} \quad (|\dot{q}|)^2 e^{-\hat{T}_0 |\dot{q}|}] \\ \Psi &= [\alpha_1 \quad \alpha_2 \quad \alpha_3 \quad \alpha_4]^T \end{aligned}$$

Adaptation to the upper bounding function

The estimate $\hat{\rho}$ of the upper bounding function is

$$\hat{\rho} = \mathbf{X}\hat{\Psi} \tag{18}$$

where the parameter estimates in $\hat{\Psi}$ are updated according to

$$\dot{\hat{\Psi}} = \mathbf{\Omega}_2 \mathbf{X}^T |r| \tag{19}$$

where $\mathbf{\Omega}_2 \in \mathbf{R}^{4 \times 4}$ is a diagonal matrix with positive gains.

To summarize, the smooth adaptive robust friction compensating algorithm consists of controller (11) together with the adaptation laws (12), (18) and (19). Adaptive law (10) is substituted for the $\hat{\tau}_{st}$ update in (12) when there is no motion.

5. STABILITY THEOREM AND ANALYSIS

Lemma

There exist constants $\alpha_1, \alpha_2, \alpha_3$ and α_4 such that the ρ in equation (16) forms an upper bounding function satisfying (15) for all $\beta_1, \beta_2, \beta_3, \tau_e$ and T_0 and all possible a priori estimates for these constants.

Proof. By expanding $e^{\tilde{T}_0 |\dot{q}|}$ in a Taylor series about zero velocity, equation (14) can be written as

$$\omega = -\beta_1 \sin(\beta_2 q + \beta_3) + \operatorname{sgn}(\dot{q}) \{ -\tilde{\tau}_e + \tilde{\tau}_e e^{-\hat{T}_0 |\dot{q}|} - \tau_e \tilde{T}_0 |\dot{q}| e^{-\hat{T}_0 |\dot{q}|} - \frac{1}{2} \tau_e (\tilde{T}_0 |\dot{q}|)^2 e^{-\hat{T}_0 |\dot{q}|} + \mathbf{R} \} \tag{20}$$

where R stands for the error remaining in the associated product when using only the first three terms in the expansion. The sinusoidal term in equation (20) is bounded and this bound forms part of the α_1 term. The same is true of the $\text{sgn}(\dot{q})\tilde{\tau}_e$ term. The α_2, α_3 and α_4 terms come from the corresponding terms in (20). The remainder term is bounded by

$$|R| = \left| \text{sgn}(\dot{q}) \left\{ -\tau_e \frac{1}{3!} \frac{d^3}{dx^3} \Big|_{x=x^*} (\tilde{T}_0 |\dot{q}|)^3 \right\} \right|$$

$$\leq \tau_e \frac{1}{3!} e^{-T_0 |\dot{q}|} (\tilde{T}_0 |\dot{q}|)^3$$

This bound is zero when $|\dot{q}|$ is zero, and also when $|\dot{q}|$ goes to infinity. It assumes a maximum value for some finite value of $|\dot{q}|$, and this maximum is also absorbed in α_1 , which completes the proof. □

Remark 1

The ρ in equation (16) still forms an upper bounding function satisfying (15) even in the presence of hysteresis. Hysteresis can be modelled by using different values of τ_e and T_0 in (5) between velocity reversals. As proved in the above Lemma, ρ in equation (16) forms an upper bounding function satisfying (15) for all τ_e and T_0 .

Theorem

The servo system (4) is globally asymptotically stable under the controller (9) with adaptation laws (10), (12) and (19), i.e., the position tracking error converges to zero as $t \rightarrow \infty$.

Proof. Choose the Lyapunov function candidate

$$V(r, \tilde{\Phi}, \tilde{\Psi}) = \frac{1}{2} Jr^2 + \frac{1}{2} \tilde{\Phi}^T \Omega_1^{-1} \tilde{\Phi} + \frac{1}{2} \tilde{\Psi}^T \Omega_2^{-1} \tilde{\Psi} \tag{21}$$

This is a globally positive definite function of its variables, which is continuous and differentiable with respect to its arguments, and hence with respect to time.

The derivative of V along the system trajectory (13) is

$$\begin{aligned} \dot{V} &= rJ\dot{r} + \tilde{\Phi}^T \Omega_1^{-1} \dot{\tilde{\Phi}} + \tilde{\Psi}^T \Omega_2^{-1} \dot{\tilde{\Psi}} \\ &= r \{ -Br - K_D r - k_{vis} r + \mathbf{Y} \tilde{\Phi} + \omega - \hat{\rho} K_T \tanh[(a + bt)r] \} - \tilde{\Phi}^T \mathbf{Y}^T r + \tilde{\Psi}^T \mathbf{X}^T |r| \\ &= -(B + K_D + k_{vis})r^2 + r \mathbf{Y} \tilde{\Phi} + r\omega - r \hat{\rho} K_T \tanh[(a + bt)r] - r \mathbf{Y} \tilde{\Phi} + \tilde{\Psi}^T \mathbf{X}^T |r| \\ &\leq -(B + K_D + k_{vis})r^2 + |r| |\omega| - r \hat{\rho} K_T \tanh[(a + bt)r] + |r| \tilde{\Psi}^T \mathbf{X}^T \\ &\leq -(B + K_D + k_{vis})r^2 + |r| \mathbf{X} \tilde{\Psi} + |r| \mathbf{X} \tilde{\Psi} - |r| \hat{\rho} K_T \tanh[(a + bt)|r|] \\ &= -(B + K_D + k_{vis})r^2 - |r| \hat{\rho} \{ K_T \tanh[(a + bt)|r|] - 1 \} \end{aligned} \tag{22}$$

Note that

$$K_T \tanh[(a + bt)|r|] - 1 \geq 0 \tag{23}$$

if and only if

$$|r| \geq \gamma \tag{24}$$

where

$$\gamma = \frac{1}{2(a+bt)} \ln \left(\frac{K_T + 1}{K_T - 1} \right) \quad (25)$$

Furthermore, when (24) is satisfied (23) is a continuous monotonically increasing function of $|r|$.

Given any $\varepsilon \geq 0$, then if $|r| \geq \varepsilon$ and $|r| \geq \gamma$ for all time, then there exists a $\sigma > 0$ such that $\dot{V} \leq -\delta$ for all time. Integrating $\dot{V} \leq -\delta$ with respect to time produces a V that becomes negative in finite time, which is a contradiction of the positive definite property of V . Therefore, $|r|$ cannot remain larger than both γ and ε . Furthermore based on $K_T > 1$, it can be easily shown from (25) that as $t \rightarrow \infty$, $\gamma \rightarrow 0$, so that $|r|$ cannot remain larger than epsilon, no matter how small the ε . We conclude that $|r|$ approaches zero as $t \rightarrow \infty$. One can show using the definition of r and BIBO stability properties, that as r approaches zero e must also approach zero,⁵ and this completes the proof of global asymptotic convergence to zero tracking error. \square

Heuristically, $|r|$ converges to a closed ball centred at the origin with a radius of γ , and this radius tends to zero. Once $|r|$ converges to a closed ball centred at the origin with zero radius of γ , the system is on the sliding surface and converges to zero error.

Remark 2

The proposed robust compensator employing a hyperbolic tangent function is continuously differentiable with both time and the control variable, thus it has the advantage over bang–bang type and saturation type robust compensators, of producing a smooth control input.¹² Furthermore, the time-varying nature of the proposed robust compensator ensures asymptotic stability of the closed-loop system. Therefore, positioning inaccuracy and motion intermittence, two common problems associated with stick–slip friction, are avoided during the control process.

Remark 3

From the definition of r in equation (8), the relation $r \approx \lambda e$ is satisfied when the velocity of the rotor approaches zero. The robust compensator employing the hyperbolic tangent function then takes the form $\hat{\rho} K_T \tanh[(a+bt)\lambda e]$. Consider the graph of the hyperbolic tangent function, in a small neighbourhood of $e = 0$ it is similar to that of a high gain proportional controller. Therefore, $\hat{\rho} K_T \tanh[(a+bt)r]$ behaves like a high-gain proportional controller near $(e = 0, \dot{e} = 0)$ for a certain value of $(a+bt)$. Based on the fact that $\hat{\rho}$ upper-bounds the maximum static friction, the $\hat{\rho} K_T \tanh[(a+bt)\lambda e]$ robust compensator can always produce a torque exceeding the maximum static friction by properly choosing a and λ according to the desired accuracy.

Remark 4

It is worthwhile to point out that the time-varying hyperbolic tangent controller $\tanh[(a+bt)r]$ behaves smoothly even as $t \rightarrow \infty$. One might think that as time gets large, this hyperbolic function approaches a bang–bang function of r . However, as t gets large, $|r|$ approaches γ , and γ decays as the reciprocal of $(a+bt)$ according to (25). Thus, no bang–bang action is produced in the limit.

Table I. The real values and the estimates of motor and friction parameters

	J (kg m ²)	B (N m s/rad)	τ_{st} (N)	k_{vis} (N m s/rad)	τ_e (N)	T_0
Real	2.0	10	1.5	7.5	0.4	10
Estimates	1.0	20	1.0	5.0	0.35	30

Remark 5

The controller parameters a and b determine the converging rate of γ as well as the control errors during a finite time. Therefore, in practice, appropriate values of a and b can be chosen according to the required error converging rate and control accuracy.

Remark 6

The control method developed here is able to ensure the global asymptotic stability of the closed-loop system in the presence of friction hysteresis since the ρ in equation (16) still forms an upper-bounding function satisfying (15) in the presence of hysteresis.

6. NUMERICAL SIMULATIONS

In order to illustrate the efficacy of the proposed control method, numerical simulations were performed of a DC motor with both uncertain parameters and stick–slip friction.

The DC motor was required to follow the desired trajectory given as $q^d = 0.2 \cos(5t) - 0.2$. The motor parameters in system model (4) and the friction parameters in friction model (5) were unknown to the control designers (assuming the joint friction is not position dependent). The real values and the estimates are listed in Table I. In addition, the parameters for the position-dependent friction are given as $\beta_1 = 0.35$, $\beta_2 = 0$ and $\beta_3 = 0.5$.

Figure 3 shows the behaviour of a PD controller in responding to the sinusoidal desired trajectory. The proportional and derivative gains are, respectively, 10 and 2.5. The relatively small proportional control gain results in totally unacceptable tracking of the desired command. When a larger gain is used, the error becomes smaller, but the same properties still apply. Sticking still cuts off the peaks in the figure, which occur near zero velocity.

Figure 4–7 present the results of using the smooth adaptive robust controller in place of the PD controller. The λ in (8) and K_T in (9) are designed to be 4 and 2.5 so that the same PD gains as in Figure 3 are still being used in the $K_D r$ term of this controller. Both the desired trajectory and the trajectory resulting from using this new controller during the 10-second simulation period are shown, and the response is so good that they cannot be distinguished to graphical accuracy. Hence, in Figure 5 and 7 we expand the scales to be able to observe the initial small error, and to show the speed of convergence to zero tracking error. The superiority of the new smooth adaptive robust control shown in Figure 4–7 benefits from the fact that $\tanh[(a + bt)r]$ functions like a high gain proportional control in the vicinity of zero velocity.

Figure 8 shows the friction torque and the torque generated by the new control law. The parameter adaptation histories are shown in Figure 9. The rotor inertia and the breakaway

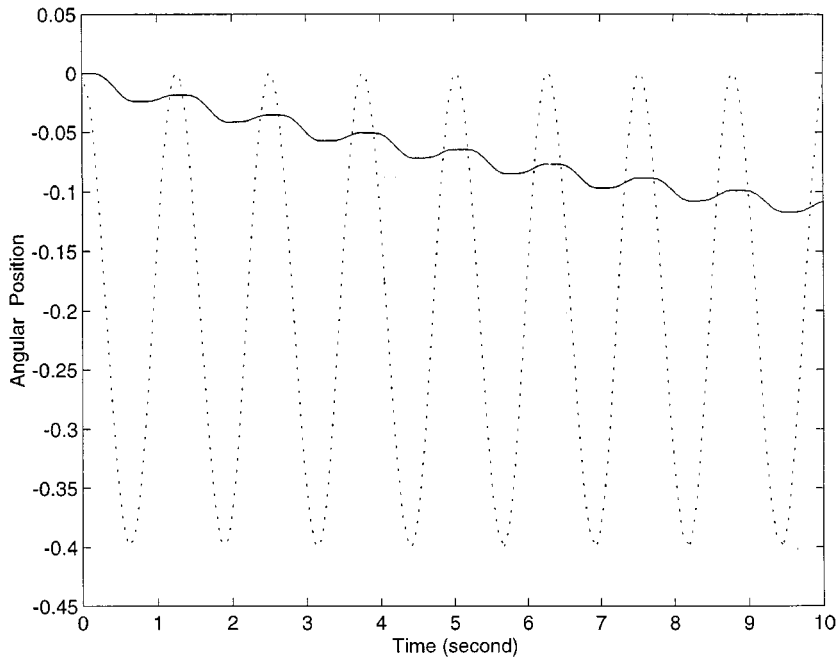


Figure 3. The effect of sticking in PD control; dotted line: desired trajectory; solid line: actual response

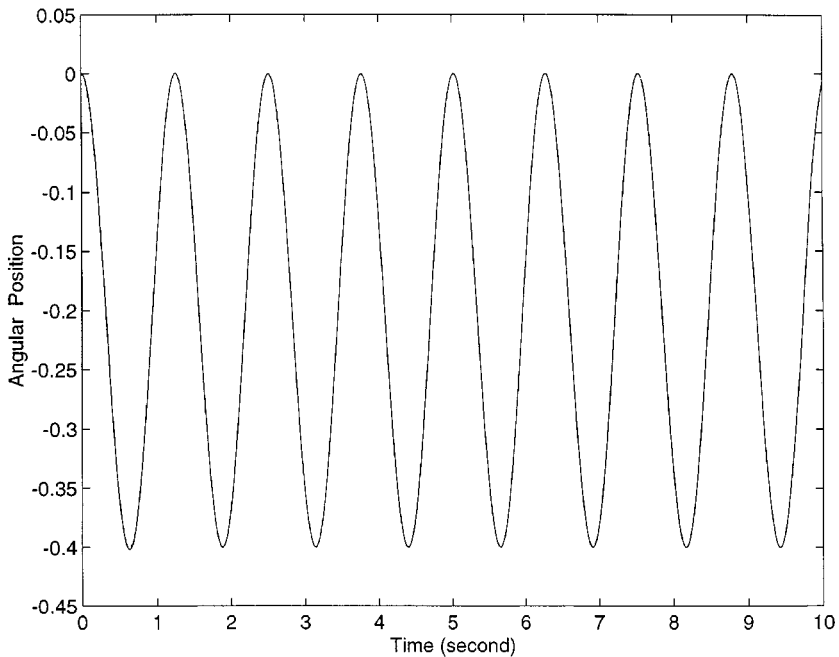


Figure 4. Angular position of the rotor when using the smooth robust controller. (Note that the desired and actual position coincide to graphical accuracy). Dotted line: desired position; solid line: actual response

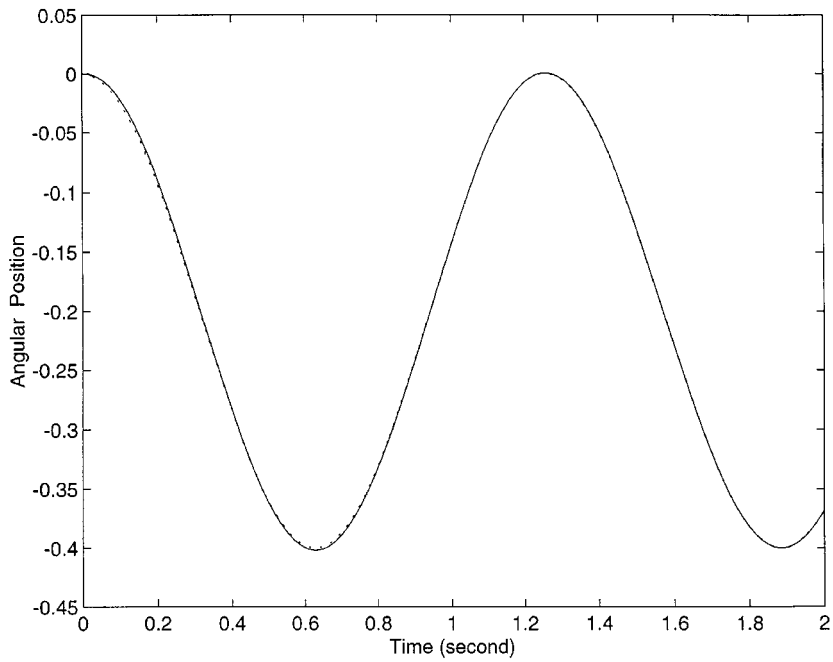


Figure 5. Expanded view of Figure 4 showing the convergence to the desired trajectory; dotted line: desired position; solid line: actual response

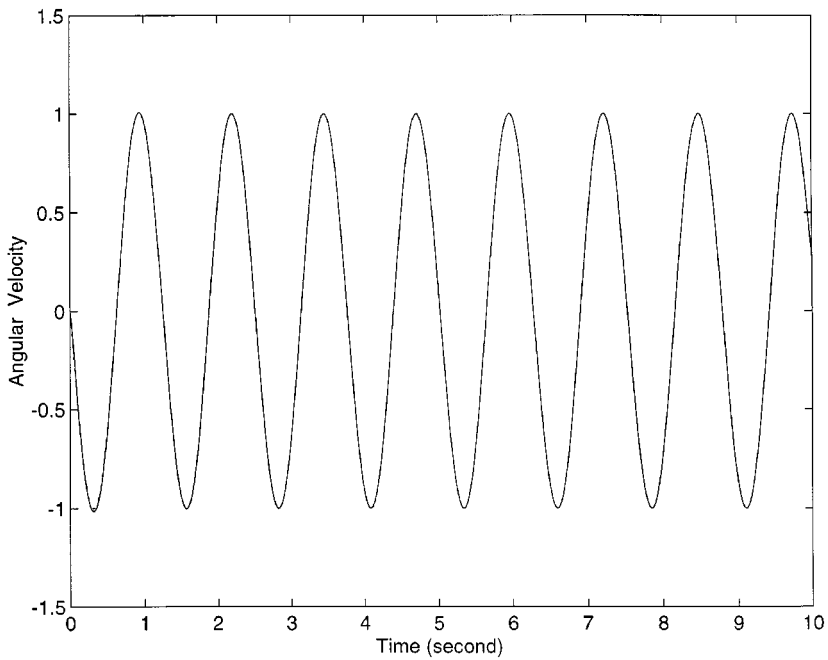


Figure 6. Angular velocity of the rotor when using the smooth robust controller. (Note that the desired and actual velocity coincide to graphical accuracy). Dotted line: desired velocity; solid line: actual response

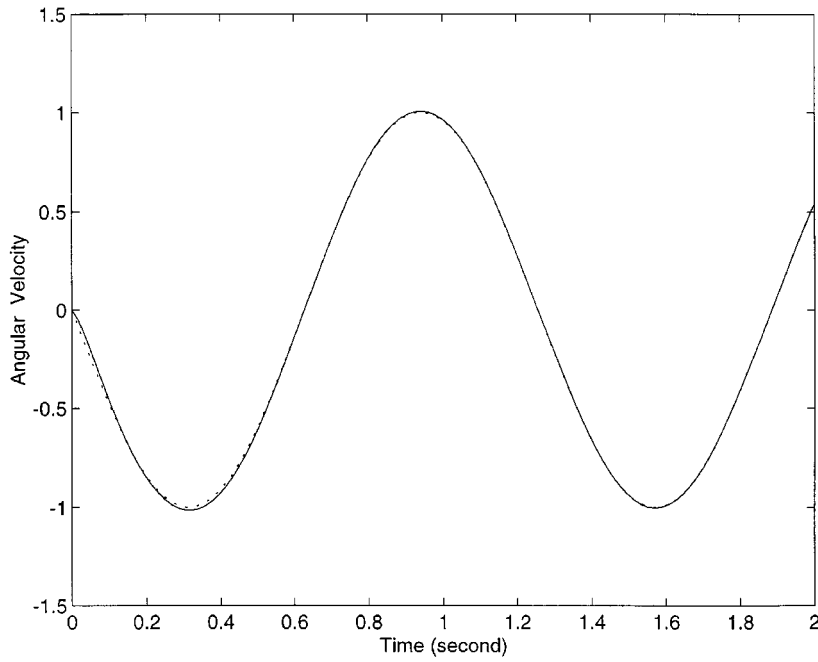


Figure 7. Expanded view of Figure 6 showing the convergence to the desired velocity; dotted line: desired velocity; solid line: actual response

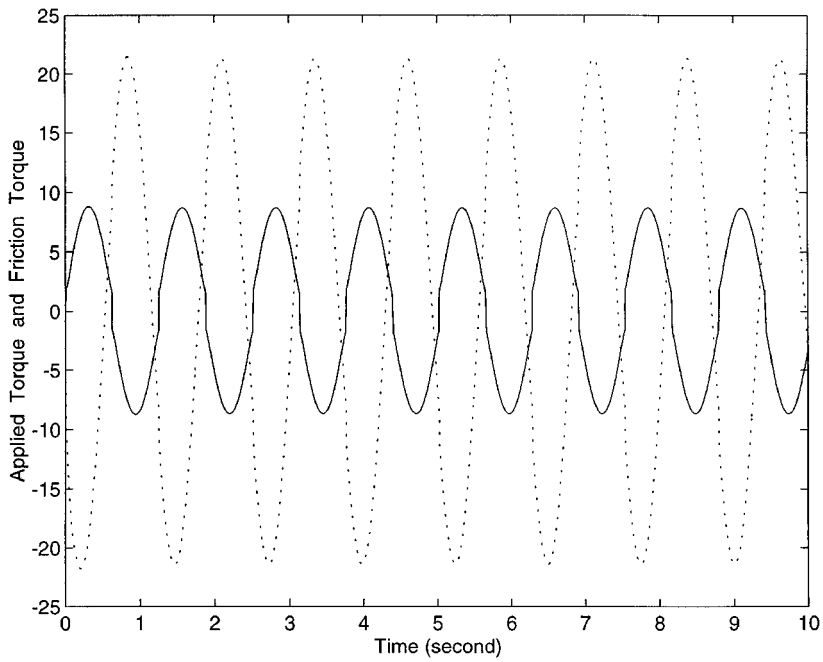


Figure 8. Friction torque and applied torque; dotted line: applied torque; solid line: friction torque

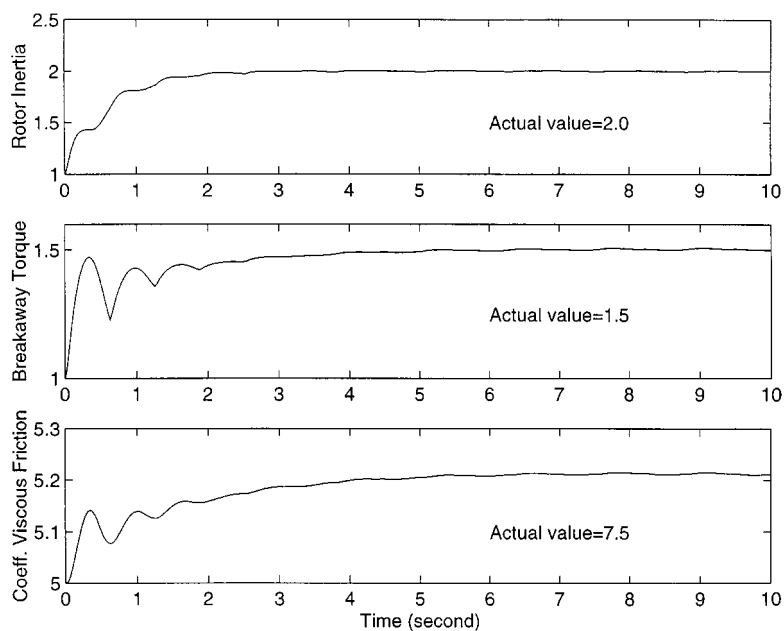


Figure 9. Parameter adaptation

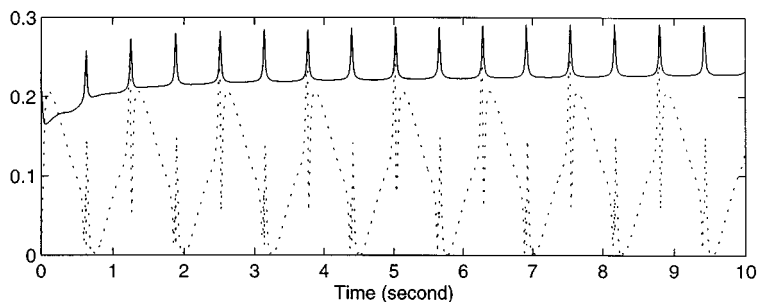


Figure 10. Adaptation of the upper-bounding function bounding the uncertainty of position-dependent friction and the uncancelled residual of the exponential friction; dotted line: uncertainty; solid line: upper-bounding function

torque estimates converge to their real values. The derivative action in the controller behaves like viscous friction, and the estimate of the viscous friction coefficient converges to a number different from the true value.

The adaptation of the upper-bounding function which bounds the uncertainty due to the inexact cancellation of the exponential torque is presented in Figure 10. We see that the upper bounding function soon bounds the uncertainty through adaptation of parameters α_1 , α_2 , α_3 and α_4 . Therefore, stability of the system is guaranteed.

7. CONCLUSIONS

In this paper, a new approach employing a smooth adaptive robust controller has been developed for tracking control of a servo-system with stick-slip friction. This controller is sliding-mode

based, and consists of three parts: feedforward terms computed based on estimated knowledge of both the servo-system and the friction model, a linear feedback force, and a robust compensator. The portion of feedforward terms which are linear or linear in parameters are updated during the control process according to an adaptive algorithm. Meanwhile, a robust compensator is used to compensate for the uncertainties due to inexact cancellation of the terms which are neither linear nor linear in parameters, e.g., the exponential friction component used to capture the downward bend of the friction torque at low velocity and the sinusoidal friction component describing the position-dependent friction torque. The robust compensator employs an adaptive algorithm to 'learn' the upper-bounding function on line. Thus, no prior information is required. Moreover, the robust compensator is smooth in the sense that it is continuously differentiable with both time and the control variable. Lyapunov's direct method has been used to prove the global asymptotic stability of the closed-loop system. Numerical simulations have demonstrated the effectiveness of the proposed controller to compensate for stick-slip friction. Experimental verification of the proposed friction compensation method is considered to be a future task.

REFERENCES

1. Southward, S. C., C. J. Radcliffe and C. R. MacCluer, 'Robust nonlinear stick-slip friction compensation', *J. Dynamic Systems, Measurement, and Control*, **113**, 639–645 (1991).
2. Canudas de Wit, C. and V. Loand Seront, 'Robust adaptive friction compensation', *Proceedings of IEEE Inter. Conf. Robotics and Autom.*, Cincinnati, Ohio, 1990, pp. 1383–1388.
3. Cai, L. and G. Song, 'A smooth robust nonlinear controller for robot manipulator with joint stick-slip friction', *Proceedings of IEEE Inter. Conf. Robotics Autom.*, Atlanta, GA, 1993, pp. 449–454.
4. Cai, L. and G. Song, 'Jointstick-slip friction compensation of robot manipulators by using smooth robust controllers', *J. Robotic Systems*, **11**(6), 451–470 (1994).
5. Slotine, J.-J. E. and W. Li, 'On the adaptive control of robot manipulators', *Int. J. Robotics Research*, **6**(3), 49–59 (1987).
6. Cai, L. and A. Abdalla, 'A smooth tracking controllers for uncertain robot manipulator', *Proceedings of IEEE Inter. Conf. Robotics Autom.*, Atlanta, GA, 1993, pp. 83–88.
7. Stribeck, R., 'Die wesentlichen eigenshaten der gleit und rollenlager' (the key qualities of sliding and roller bearings), *Zeitschrift des Vereines Seutscher Ingenieure*, **46**(38–39), 1342–1348, 1432–1437 (1902).
8. Armstrong-Helouvry, B., 'Stick-slip arising from Stribeck friction', *Proceedings of IEEE Int. Conf. Robotics and Autom.*, Cincinnati, OH, 1990, pp. 1377–1382.
9. Tustin, A., 'The effects of backlash and of speed-dependent friction on the stability of closed-cycle control system', *J. Institute of Electrical Engineers*, **94**(2A), 143–151 (1947).
10. Gomes, S. C. P. and J. P. Chretien, 'Dynamic modeling and friction compensated control of a robot manipulator joint', *Proceedings of IEEE Inter. Conf. Robotics and Autom.*, Nîle, France, 1992, Vol. 3, 1429–1435.
11. Lewis, F. L., C. T. Abdallah and D. M. Dawson, *Control of Robot Manipulators*, Macmillan Publishing Company, New York, 1993.
12. Song, G., 'Robust control and adaptive robust control of robot manipulators', Ph.D. Dissertation, Department of Mechanical Engineering, Columbia University, 1995.
13. Canudas, C., K. J. Astrom and K. Braun, 'Adaptive friction compensation in DC-motor drives', *IEEE J. Robotics and Autom.*, **RA-3**(6), 681–685 (1987).
14. Karnopp, D., 'Computer simulation of stick-slip friction in mechanical dynamic system', *J. Dynamic Systems, Measurement, and Control*, **107**, 100–103 (1985).
15. Song, G., A. Abdalla, L. Cai and Y. Wang, 'Stick-slip friction compensation of uncertain robot manipulators using neural network controllers', *Preprints of IFAC International Symposium of Robot Control*, Capri, Italy, 1994, pp. 973–978.
16. Spong, M. W. and M. Vidyasagar, *Robot Dynamics and Control*, Wiley, New York, 1989.
17. Vidyasagar, M., *Nonlinear Systems Analysis*, Prentice-Hall, New Jersey, 1978.
18. Walrath, C. D., 'Adaptive bearing friction compensation based on recent knowledge of dynamic friction', *Automatica*, **20**(6), 717–727 (1984).